[37] Walburn, A. B., "An Analytical and Experimental Examination of the Effect of Cryogenic Propellant Venting on Orbital Vehicle Dynamic Behavior," American Astronautical Society Southeastern Symposium in Missiles and Aerospace Vehicles Sciences, Dec. 1966.

[38] Rod, R. L., Knox, C., and Doshi, N. H , "Propellant Utilization and Control for Spacecraft," AFRPL-TR-65-155, Sept. 1965, Air Force Rocket Propulsion Lab., Edwards, Calif.

[39] Perkins, C. K., Rivinius, F. G., and Wood, G. B., "Stillwells for Propellant Gaging," RAC-ZZD-63-011, Jan. 1964, General Dynamics/Astronautics Div., San Diego, Calif.

[40] Wright, D. E. and Honebrink, R. W., "Nucleonic Propellant Measurement System for Zero G Requirements," Rept. ER-80106 July 1, 1963, Giannini Controls Corp.

[41] Wright, D. E., "Nucleonic Propellant Gaging and Utilization Systems for Space Vehicles," private correspondence, July 1, 1963, Giannini Control Corp.

[42] "Molimetric Propellant Gaging System," Rept. PD 1152, Sept. 15, 1966, Simmonds Precision Products.

[43] Gronner, A. D., "Methods of Gaging Fluids Under Zero-G Conditions," *7th Liquid Propulsion Symposium*—Vol. I, Oct. 1965, pp. 311–340.

[44] Boretz, J. E. et al., "Ultra-Low-Pressure Rocket (ULPR) Propulsion System—Phase I, Summary Report, Final, Vol. I, Technical Report," AF Contract AFO4 (611)-7434, ASTIA 327828, Feb. 1962, Denver Div., Martin-Marietta.

[45] Macklis, H., Wakeman, J., and Boretz, J. E., "MOL Propellant Gauging System," Rept. S/N 6391.000, Feb. 1966, TRW.

[46] Burington, R. S. and Torrance, C. C., *Higher Mathematics*, McGraw-Hill, New York, 1939.

[47] Chi, J. W. H., "Forced Convective Boiling Heat Transfer to Hydrogen," *Journal of Spacecraft and Rockets*, Vol. 3, No. 1, Jan. 1966, pp. 150–152.

[48] Robbins, J. H. and Rogers A. C., Jr., "An Analysis of Predicting Thermal Stratification in Liquid Hydrogen," *Journal of Spacecraft and Rockets*, Vol. 3, No. 1, Jan. 1966, pp. 40–45.

[49] Vliet, G. C., "Stratification with Bottom Heating," *Journal of Spacecraft and Rockets*, Vol. 3, No. 7, July 1966, pp. 1142–1145.

[50] Stephens, D. G., "Flexible Baffles for Slosh Damping," *Journal of Spacecraft and Rockets*, Vol. 3, No. 5, May 1966, pp. 765–766.

[51] Gronner, A. D., "Methods of Gaging Fluids under Zero-G Conditions," *Journal of Spacecraft and Rockets*, Vol. 3, No. 7, July 1966, pp. 1058–1062.

[52] Kenny, R. J. and Friedman, P. A., "Chemical Pressurization of Hypergolic Liquid Propellants," *Journal of Spacecraft and Rockets*, Vol. 2, No. 5, Sept.–Oct. 1965, pp. 746–753.

[53] Reeves, D. F., "Volatile Liquid Pressurization Control System," *Journal of Spacecraft and Rockets*, Vol. 2, No. 5, Sept.–Oct. 1965, pp. 795–797.

[54] Cody, E. C., "An Investigation of Fluorine-Hydrogen Main Tank Injection Pressurization," *Journal of Spacecraft and Rockets*," Vol. 6, No. 11, Nov. 1969, pp. 1248–1253.

[55] Burge, G. W., Blackmon, J. B., and Madsen, R. A., "Analytical Approaches for the Design of Orbital Refueling Systems," AIAA Paper 69-567, U.S. Air Force Academy, Colo., 1969.

[56] Wood, C. C. and Trucks, H. F., "Evaluation of Experimental and Analytical Data for Orbital Refueling Systems," AIAA Paper 69-566, U.S. Air Force Academy, Colo., 1969.

[57] Morgan, L. L., "Parametric Studies of Orbital Fluid Transfer," AIAA Paper 69-565, U.S. Air Force Academy, Colo., 1969.

MAY 1970 J. SPACECRAFT VOL. 7, NO. 5

Vacuum Startup of Reactors for Catalytic Decomposition of Hydrazine

H. GREER*
The Aerospace Corporation, El Segundo, Calif.

Experimental results characterizing the first-pulse startup of monopropellant hydrazine thrusters, using a spontaneous catalyst (Shell 405), are presented and analyzed. Typical reactor dynamics are presented as approximations in simulating spacecraft control system dynamics. Possible reasons for first-pulse pressure spiking are explored as an approach toward controlling or alleviating catalyst attrition. Among the variables investigated are injector/catalyst configuration and initial temperature, vacuum exposure time and catalyst degassing, thrust level, and water immersion. Potential problems of propellant valve leakage and injector clogging are discussed. Several apparent trends are postulated from the test results, but additional study is needed for a clear understanding of the mechanisms involved.

Nomenclature

C_p = heat capacity of liquid
D = diameter
H_f = heat of fusion
H_v = heat of vaporization
m = molecular weight
P = pressure
R = universal gas constant
T = temperature
V = volume
$\dot{W}$ = weight flowrate
w = weight
X = the quantity of propellant entering the vapor phase = $(H_f + C_p\Delta T)/(H_v + H_f)$
θ = time

Subscripts

a = ambient
c = reactor chamber (T_c or P_c) or command (θ_c)
f = fluid
i = injector or ignition delay

Received January 28, 1970. This work was performed under Air Force Contract F04701-69-C-066. The author is grateful to D. J. Griep and F. W. Cox of the Electronics Division for their assistance in conducting the experimental program, and to H. Takimoto, Chemical Propulsion Lab., Aerospace Corp., for his help with the injector clogging problem.

* Member of the Technical Staff, Applied Mechanics Division. Associate Fellow AIAA.

Introduction

THE development of a spontaneous catalyst (Shell 405) made monopropellant hydrazine propulsion more attractive for many applications. Because data on N_2H_4 thruster operation with this catalyst in a space environment is meager, experiments have been performed in reactors (Fig. 1) to a) identify mechanisms which might be involved in the spikes during startup as the first step toward improving first-pulse operation, b) provide a better understanding of the general dynamic characteristics of typical monopropellant N_2H_4 reactors, and c) establish approximate trends for use in simulating spacecraft control system dynamics.

Reactor Configurations and Instrumentation

The tests were performed with a 0.12-lbf and a 1.7-lbf thruster. Reactors for the 0.12-lbf thruster were constructed from both aluminum and Pyrex-lined Lucite. The transparent chamber was designed to permit high-speed color movies to be taken of the injection-ignition process. The aluminum chamber provided better utility as a laboratory unit and was consequently used for the 1.7-lb thruster, Fig. 2. Each reactor comprised a N_2H_4 reservoir pressurized by N_2 gas, a propellant solenoid valve, a single-orifice injector, a bed of Shell 405 catalyst supported by a 60-mesh screen welded to an instrumentation spacer and conical, 15° half-angle, nozzle with an expansion ratio of 48 or 50 (see Table 1).

With the 0.12-lbf reactor, tests were performed both without screens and with screens placed between the injector orifice and a 14–18 mesh catalyst bed. Three screen configurations were tested; in two configurations a screen (40 and 120 mesh) was installed flush between the injector and the catalyst; and in the third configuration a 40-mesh screen was positioned downstream of the injector, resting on the catalyst, to create a screen void space amounting to approximately 10% of the empty reaction chamber.

The following catalyst configurations were tested in the 1.7-lbf aluminum thruster; configuration A, used homogeneous 14–18 mesh without screens; configuration B, new homogeneous 14–18 mesh with a 60-mesh screen at the injector face and another 60-mesh screen 0.2-in. below the first, and with 14–18 mesh catalyst between the screens; configuration D, new 25–30 mesh catalyst between 60-mesh screens 0.2 in. apart at the injector face with new 8–12 mesh catalyst in the lower bed; and configuration E, in which the 25–30 mesh catalyst, normally contained in the 0.2-in. layer between the screens, was homogeneously blended with 8–12 mesh catalyst and used without screens.

Table 1 Thruster design characteristics (at an assumed gas temperature of 135°F)

Estimated thrust, F, lb	0.12	1.7
Downstream chamber pressure, P_c, psia	75	160
Nozzle expansion ratio, ϵ	48	50
Assumed nozzle coefficient, C_f	1.73	1.73
Estimated specific impulse, I, sec	125	125
Nozzle throat diameter, D_t, in.	0.035	0.088
Nozzle exit diameter, D_e, in.	0.24	0.62
Flow rate, $\dot{W}$, lb/sec	0.001	0.014
Chamber diameter, D_c, in.	0.35	0.51
First catalyst layer, mesh size	14–18	25–30 [a]
Second catalyst layer, mesh size	...	8–12 [a]
Total catalyst bed length, in.	1.25	1.58
Total chamber length, in.	1.75	2.10
Type of injector	Single orifice	Single orifice (with screen)
Injector orifice diameter, D_i, in.	0.0082	0.024
Reservoir pressure, P_r, psia	115	315
Total catalyst weight, g	2.7	6.7
Catalyst bed loading, G, lb/sec-in.^{2}	0.01	0.07
Calculated residence time, θ_r, msec	5	1

[a] Corresponds to configuration D.

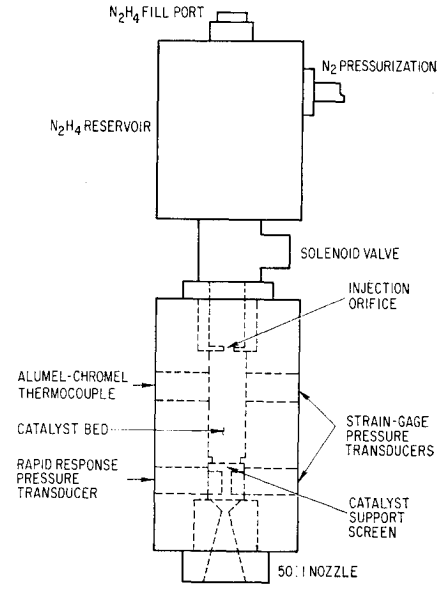

Fig. 1 Schematic of monopropellant N_2H_4 reactor.

A high-response Kistler transducer was used to measure peak spiking pressure downstream of the catalyst bed. A standard controls (strain-gage) transducer obtained the chamber pressure profile which was not available with the Kistler transducer. The conditioned outputs of the two pressure transducers, the solenoid valve coil current, and the thermocouple in the catalyst bed were simultaneously displayed on a oscilloscope and photographed.

One probe of a dual-head Pirani gage was installed in the reactor at the end of the catalyst bed just upstream of the nozzle, and the other was located in the vacuum chamber. Gas desorption from the catalyst surface was indicated by the pressure difference between the two probes.

A chromel-alumel thermocouple, mounted in the catalyst bed 0.5 in. downstream of the injector orifice, was used to monitor average catalyst bed temperature T_c. The

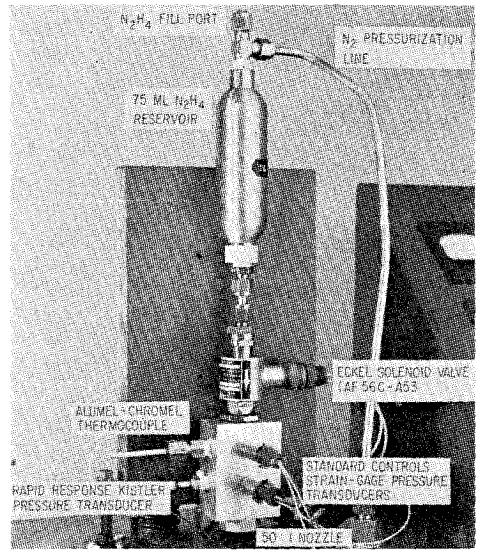

Fig. 2 1.7-lb-thrust reactor.

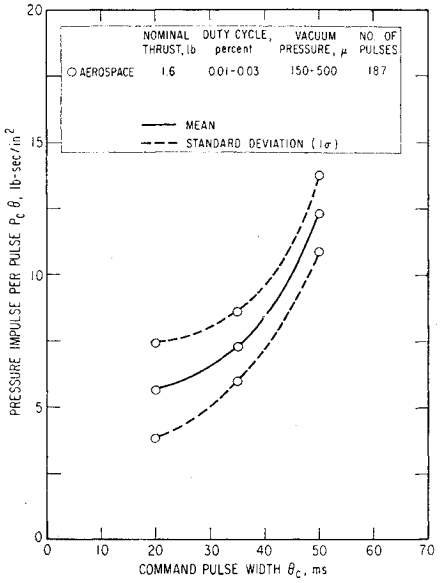

Fig. 3 Pressure impulse repeatability.

solenoid valve circuitry used a dual preset counter to provide the desired valve command pulse duration and a two-stage transistor power amplifier to actuate the valve. The valve coil current was monitored by a sampling resistor in series with the valve coil and current profiles were monitored for all short-pulse firings made. An electric resistance heater was wrapped around the reactor; and an on-off control system having a ±3°F deadband held the catalyst temperature at the desired value.

Impulse Repeatability

Pressure impulse repeatability was studied with the 1.7-lbf thruster using catalyst configuration D; 187 vacuum firings were made at 3-min intervals using command pulse widths of 20, 35, and 50 msec. Pressure impulse areas (psi-sec) were computed automatically and printed out. Oscilloscope traces of valve coil-current, T_c, and P_c provide direct data illustrating starting characteristics, repeatability, shutdown, and small-pulse-bit characteristics. The coil current traces indicated a flux buildup time (electrical delay) of approximately 4.4-msec and a proppet travel time of about 0.5 msec. The feed-line hydraulic delay was not specifically measured, but its effect was limited by minimizing the distance from the valve to the injector. The injector orifice in these tests was located right at the valve discharge, Fig. 1, minimizing propellant holdup in the injector.

The impulse delivered per pulse is a function of the command pulse width θ_c, pulse frequency, and P_c. The average flow rate for short pulses is higher than for longer pulses, since the injector pressure drop is larger before P_c builds up. The heat lost during heating of the catalyst bed and the engine mass reduces impulse bit-size for single pulses, short pulses, and first pulses. For the reactor configuration and the duty cycles (0.01%–0.03%) tested, T_c appeared to stabilize at about 240–250°F, so that variation in impulse due to thermal effects was small.

The pressure impulse delivered per pulse is shown in Fig. 3 together with standard 1-σ deviation, as a function of θ_c. Pressure impulse (the area under the pressure trace) was selected for two reasons: it was a measured parameter, and it permits comparison with data obtained for motors of different thrust levels. As expected, the impulse repeatability improved as θ_c increased; the standard deviation decreased from 32% to 12% as θ_c increased from 20 msec to 50 msec.

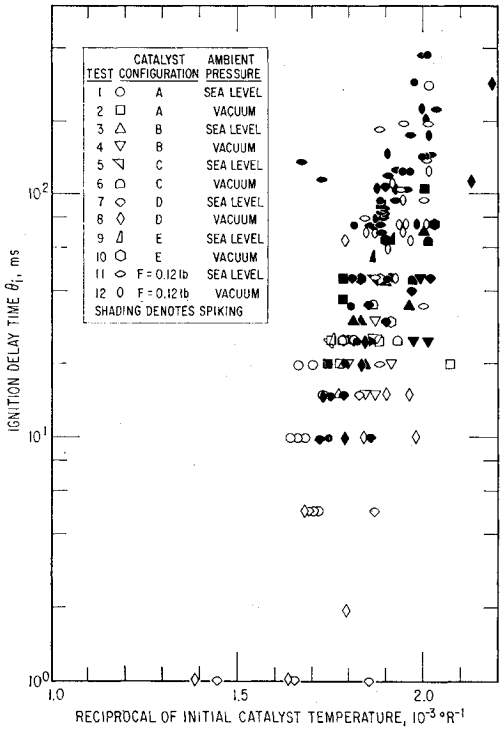

Fig. 4 Effect of catalyst temperature T_c on ignition delay time θ_i.

Vacuum Exposure Time and Injector Configuration

Vacuum ignition, 75°F, pressure spiking tests were made using both transparent Lucite and aluminum reaction chambers in the 0.12-lbf thruster. One series of tests used a single orifice injector while the other series of tests used three different injection screen configurations. A total of 1391 hr of vacuum exposure time were accumulated during 168 tests, and spiking was observed in approximately 22% of the firings.

To see if there could be a relation between ignition delay θ_i and pressure spiking, average θ_i's, with and without spiking, were compiled for each injector/screen type and reactor material. Although spiking occurred with each configuration, there was an apparent increase in θ_i (with spiking) for the aluminum reactor as compared to the Lucite reactor. This increase could be attributed to greater thermal conductivity of the metal, which might tend to absorb more heat and somewhat quench the reaction. Except the data from the fine mesh screen configuration, the average θ_i with spiking appeared to be greater than without spiking,† Fig. 4.

An estimate of the upper magnitude of such a spike was obtained by assuming closed-volume combustion, i.e., full injector flow during the ignition delay time, complete and instantaneous decomposition at the end of the delay, and no thrust nozzle outflow. Under these conditions, $P_c = \dot{W}_i\theta_i RT/mV_c$. If a θ_i of 10 msec is assumed, a maximum P_c of three times the design value could be produced in the configurations tested. Evidently, the foregoing equation oversimplifies the problem. First of all, the decomposition does not occur instantaneously in a closed volume. Secondly, cavitation and two phase flow in the injector could significantly limit $\dot{W}_i$ during vacuum starting. And finally, gaseous, liquid, or solid material (propellant, reaction intermediates or products)

† This effect has also been reported in Ref. 2.

Table 2 Effect of N_2H_4 temperature (configuration D, F = 1.7 lb)

Initial T_c, °F (N_2H_4 temperature = 75°F)			<36		36 to 69		70 to 95		>95		All	
			S.L.	Vac.	S.L.	Vac.	S.L.	Vac.	S.L.	Vac.	S.L.	Vac.
Spiking rating[a]			1/1	2/2	2/2	0/3	4/7	2/3	4/7	1/6	11/17	5/14
θ_i,[b] msec	Spiking	Yes	45	205	35	...	45	22	21	10	35	93
		No	...	...	...	13	7	10	2	15	5	14
(N_2H_4 temperature <75°F) Spiking rating[a]			0	...	2/4	...	6/7	...	1/7	...	9/18	...
θ_i,[b] msec	Spiking	Yes	0	...	55	...	66	...	30	...	49	...
		No	c	...	52	...	1	...	7	...	16	...
(All N_2H_4 temperatures) Spiking rating[a]			1/1	2/2	4/6	0/3	10/14	2/3	5/14	1/6	20/35	5/14
θ_i,[b] msec	Spiking	Yes	45	205	45	...	51	22	23	10	41	93
		No	c	...	52	13	4	10	5	15	12	14

[a] (Number of spikes)/(total number of tests).
[b] Ignition delay time, from full open to 1% of P design.
[c] Frozen N_2H_4.

might accumulate on the chamber walls or in the catalyst and later either discharge to vacuum or react in producing a spike.

Representative pulse shapes for the various configurations are shown in Fig. 5. With the head-end void configuration, the first pulses after filling the reservoir with N_2H_4 appeared to be somewhat erratic and not as repeatable as subsequent pulses. The pressure traces for all the screened injector configurations were more rounded with less low-level oscillations.

Catalyst Configuration and Temperature

One postulation was that a cold catalyst bed, together with evaporative cooling (or even supercooling) in vacuum, could cause an accumulation of N_2H_4 in the chamber (especially since the injector flow rate is highest before P_c builds up) during the ignition delay. Subsequent decomposition of the accumulated N_2H_4 might then produce pressure spiking.

The pressure in the reaction chamber increases due to evaporation of propellant. When it reaches the triple-point pressure, freezing ceases and when it reaches the vapor pressure of the liquid (14 mm of Hg), evaporation stops. The weight of undecomposed N_2H_4 vapor needed to increase the reactor pressure from 1 μ to the triple point is given by $w = PV/(RT) = 1.06 \times 10^{-8}$ lb/cm^3 of void volume. The triple-point pressure would be reached in a fraction of a millisecond with the reactor tested. Therefore, the accumulation of an excess of relatively nonreactive solid N_2H_4 crystals,‡ which could produce a severe pressure spike if simultaneously decomposed, does not appear likely.

Experiments were performed to determine the effect of catalyst configuration and temperature on θ_i and on the probability of ignition pressure spiking, using both thruster sizes. The 0.12-lbf thruster data were obtained with the aluminum reaction chamber using a homogeneous 14–18 mesh catalyst configuration and θ_c = 250 msec. The 1.7-lbf thruster was tested using the previously described catalyst configurations A–E.

Several interesting observations may be inferred from results in Fig. 4. Spiking occurred as often at sea-level as in vacuum, and it occurred more frequently at $T_c < T_a$ than at $T_c > T_a$, and $\theta_{i\text{avg}}$ was greater with spiking than without. The screened dual mesh catalyst, configuration D, appeared to be less susceptible to spiking than the other four configurations and consequently was investigated in more detail (Table 2). The unscreened homogeneous 14–18 mesh catalyst, configuration A, not only had a high spiking incidence, but produced the greatest $P_{c\max}$ when spiking occurred (Fig. 6). The typical 600-psia pressure spike obtained with configuration A at sea level with an initial T_c of 51°F is shown in Fig. 6a. Under the same conditions, a pressure spike of only 200 psia, as shown in Fig. 6b, was produced with the screened dual-mesh,§ configuration D.

Pulverization of the catalyst was observed after repeated firings in which peak spike pressures up to four times the design pressure were measured. After 12 such spikes,¶ the 14–18 mesh Shell 405 (ABG) catalyst (configuration A) was reduced to 75% < 60 mesh. Photo-micrographs (Fig. 7) show that before firing the catalyst granules are nearly uniform in size and relatively spheroidal, with a few cleavage cracks; after firing, the granules are quite disperse in size and angular in shape, suggesting that breakup was not due to hydraulic forces. It was hypothesized that pulverization (and spiking) might be due to internal pressure in the catalyst granules generated by very rapid decomposition of accumulated N_2H_4.

A possible reason that configuration D may be preferable to configuration A is that a 0.20-in. layer of fine mesh catalyst and screens provides a better distribution of smaller N_2H_4

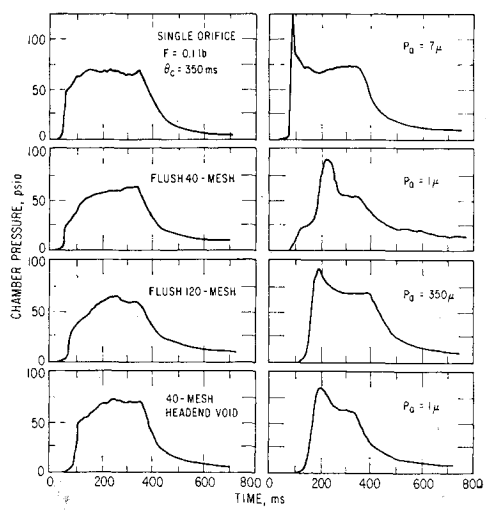

Fig. 5 Typical pressure traces.

‡ Supercooled liquid N_2H_4, produced by evaporative cooling, can exist at temperatures as low as 6°F below the freezing point. Simple catalyst activity tests, consisting of dropping a catalyst granule cooled to 30°F onto the frozen N_2H_4, indicate that after several seconds delay, gas evolution occurs and the solid N_2H_4 melts.

§ This type of configuration has been recommended[3] to reduce pressure roughness.

¶ Post-firing inspection revealed that the pulverized catalyst bed was about 75% of the original length.

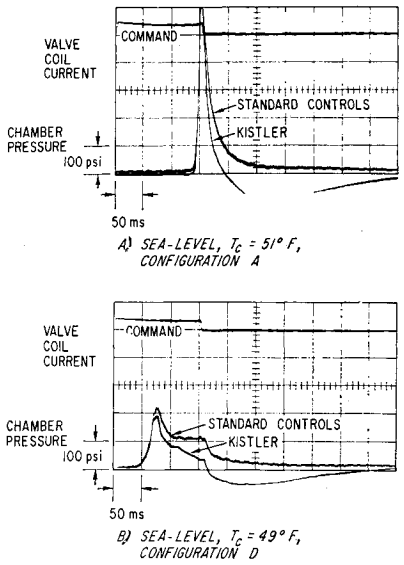

Fig. 6 Effect of catalyst configuration.

droplets and alleviates bed channeling. This improvement in flow characteristics was indicated by high-speed color movies taken of transparent reactor firings, although in both configurations fluid N_2H_4 droplets still deeply penetrated the catalyst bed.**

In configuration B, the used homogeneous 14–18 mesh catalyst of configuration A was replaced with new (as received) catalyst. This was found to have little effect on spiking incidence or θ_i.

Catalyst bed temperature significantly affected both θ_i and the magnitude of the pressure spiking, as shown in Fig. 8 for configuration A. Figure 8a was obtained at ambient conditions, while Fig. 8b was obtained with the reactor cooled to 34°F, which resulted in a peak pressure of nearly 600 psia or four times the design pressure. It was also noted that θ_i increased from about 100 msec in Fig. 8a to about 150 msec in Fig. 8b. It was observed that all the configurations tested tended to spike more at $T_c < T_a$ than at $T_c \geq T_a$. These results indicate that θ_i (required to wet the catalyst and for the initial decomposition heat release to bring some catalyst particles to a temperature at which decomposition is rapid) is strongly affected by T_c; for T_c <40°F, $\theta_i \gtrsim$100 msec.

Figure 4 also shows a general trend of increasing θ_i with decreasing T_c, but the relationship is too poorly defined to warrant an empirical mathematical expression.

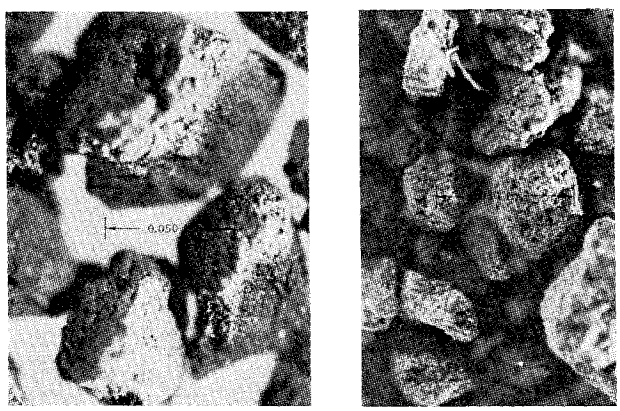

Fig. 7 Catalyst as received (left) and after spiking (right).

** Also observed in the movies were intense localized incandescent zones appearing randomly throughout the bed.

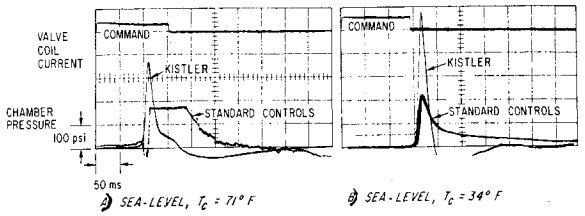

Fig. 8 Effect of catalyst temperature on spiking.

The effects of both catalyst and N_2H_4 temperature on θ_i and on the spiking characteristics of the dual-mesh catalyst (configuration D) were also investigated. The results of the vacuum tests, listed in Table 2, show that when the catalyst is cooled by chilling with liquid N_2 to somewhat below the freezing point of N_2H_4, e.g., −10°F to 0°F, the first-pulse θ_i increases to ~200 msec and spiking occurs (even though this configuration was found to be comparatively nonsusceptible to spiking at higher temperatures). On subsequent vacuum firings, with the catalyst still cooled below the freezing point of N_2H_4, no pressure traces could be obtained. When the catalyst bed was deliberately warmed to about 40°F, gas was generated in the reactor and its capability to produce normal pressure traces was restored. It was postulated that partial freezing of the N_2H_4 in the catalyst caused the large θ_i for the first-pulse case. Residual liquid N_2H_4 trapped in the injector then freezes, preventing flow into the catalyst on subsequent pulses unless the frozen N_2H_4 is melted by heating the injector.

Sea-level firings were made with the N_2H_4 cooled below ambient. In this series of tests, the initial T_c was varied from 3°F to 250°F, and the N_2H_4 temperature ranged from 42°F to 68°F. No pressure traces could be obtained when the catalyst was below the freezing point of N_2H_4. Severe pressure spiking was consistently observed for firings with 34°F $\leq T_c \leq$ 94°F. These results are also listed in Table 2.

Catalyst Outgassing

A large amount of evidence suggests that solid surface catalysis involves the adsorption of reactant molecules and that catalytic action is limited to certain active sites which constitute only a small fraction of the total surface area. Reference 4 suggests that chemisorption (involving the transfer of electrons or protons between the solid surface and the adsorbate) could be the rate-controlling step for vapor

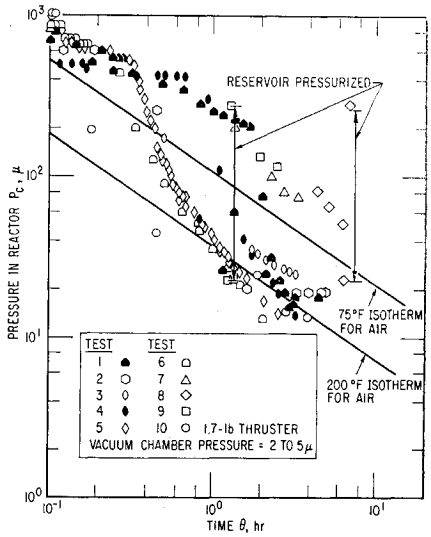

Fig. 9 Desorption after firing.

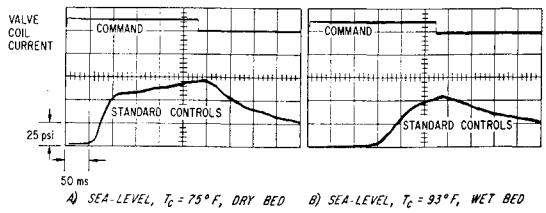

Fig. 10 Effect of water immersion.

phase N_2H_4 decomposition, whereas Refs. 5 and 6 assume that steady-state (vapor phase) N_2H_4 decomposition with a porous catalyst might be rate-limited by diffusion. In either case, activity could be affected by adsorbed nonreactive gases, which might be removed through vacuum outgassing.[4–11]

Desorption isotherms for air were obtained at constant T_c's of 75, 100, 150, and 200°F using the 0.12-lbf-thrust reactor and the electric heater. It is noted that increasing T_c increased the rate of outgassing, thereby producing lower reactor pressures at any given exposure time. These data were used to develop the constants for the following empirical expression for the desorption of air in terms of T_c (°R), P_c (μ), and vacuum exposure time θ (hr),

$$P_c = 45.6 \times 10^{14}\, T_c^{-5}\theta^{-0.7}$$

Desorption of N_2H_4 decomposition gases from the surface of the catalyst in the reaction chamber was also measured after vacuum firings of the reactors at θ_c = 250 msec. The results of 10 firings are shown in Fig. 9. A sudden jump in P_c to ~300 μ was observed in tests 8 and 9 as the propellant reservoir was pressurized to 100 psig. This sudden increase in pressure was interpreted as being an indication of valve leakage.††

The decays of P_c after firing cut across the air desorption isotherms in Fig. 9 due to the variation in T_c with time.‡‡ The unusual bump in the after-firing desorption data, observed at exposure time less than 1 hr, was attributed to the holdup and slow dribble of a small amount of N_2H_4 in the injector, and solenoid valve leakage previously mentioned.

These results are believed to have possible significance with respect to the planning of expensive ultra-high vacuum qualification tests and the identification of valve leakage as a potential major variable in the study of first-pulse vacuum ignition.

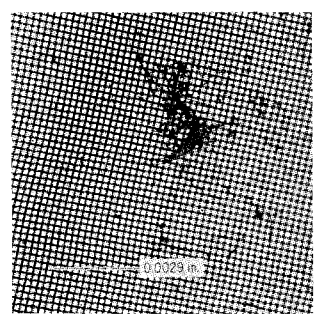

Fig. 11 Residue formed by exposure of N_2H_4 to air.

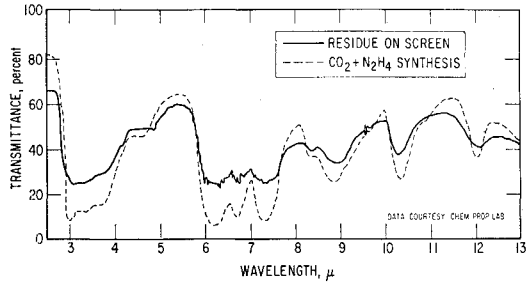

Fig. 12 Infrared spectra.

Water Immersion

The possibility that variable amounts of moisture absorption could contaminate the catalyst and affect θ_i and spiking was investigated. Chamber pressure traces were obtained before and after immersing the catalyst in water prior to firing. The P_c trace in Fig. 10a was obtained with dry catalyst at an initial T_c of 75°F. After the catalyst was immersed in water, T_c increased to 93°F, due to the heat of wetting. The P_c trace of the ensuing firing (with a wet catalyst bed) is shown in Fig. 10b; θ_i was tripled due to the water immersion, and the P_c trace was round with no indication of any tendency to spike. The pressure traces and catalyst condition on subsequent pulses appeared to be normal. Consequently, it was concluded that although moisture absorption from the atmosphere by the catalyst could increase θ_i, it probably was not the underlying cause of spiking and catalyst attrition.

Injector Clogging Problem

In the initial cold-catalyst tests of the 0.12-lbf thruster, CO_2 was used to chill the metal reactor wall. These tests were interrupted by injector clogging which could not be remedied by cleaning. Microscopic examination of the injector orifice revealed that a residue of transparent fiberous strands, such as shown in Fig. 11, was causing the clogging. Infrared spectrographs of the residue, Fig. 12, showed that it was composed of 15% C, 6% H, and 44% N. Three samples of N_2H_4 from laboratory bottles were found to contain relatively large amounts of this substance while two samples from freshly opened bottles contained only trace amounts. Subsequent experiments revealed that material,

Fig. 13 Reaction products of CO_2 + N_2H_4.

†† The effect of propellant valve leakage on P_c was estimated as follows. The maximum valve leakage rate specified for the valves used was 0.25 cm³ of liquid N_2H_4 per hr (approximately 35 standard cm³ of N_2/hr[12]) at a pressure differential of 1500 psig. For the 0.12-lbf thruster, slip flow[13] through the nozzle exists, so that the nozzle may be approximated by a cylindrical tube in using Knudsen's equation for slip flow.[14] The maximum P_c due to valve leakage at a valve pressure differential of 100 psi was found to be about 670μ, so that the actual valve leakage rate was within the maximum specification limit.

‡‡ The high-speed color movies showed incandescent catalyst particles, which are indicative of temperatures greater than 1000°F.

shown in Fig. 13, was formed by a reaction§§ between N_2H_4 and CO_2 and that a brief exposure to air was sufficient to produce it. Once formed, the fiberous substance was insoluble in either water or trichlorethylene. Cleaning the reactor was finally achieved by heating it to 275°F, at which point the clogging material sublimed completely. Liquid N_2 was then utilized for cooling the reactor; and it is recommended that N_2H_4 be handled under an inert atmosphere, such as N_2, to prevent the formation of this compound, (which could also promote the decomposition of N_2H_4 under conditions of long term storage) with the subsequent danger of blocking propellant flow in the system.

Conclusions

The dynamic characteristics of small monopropellant hydrazine reactors were measured to obtain approximations for use in simulating spacecraft control system dynamics. Impulse repeatability improved with increasing command pulse width. The results illustrate the typical loss in repeatability which might be experienced in attempting to obtain low impulse bit size by a small command pulse. A tradeoff between the effects of impulse repeatability and propellant consumption is recommended for optimum design.

The incidence and magnitude of pressure spiking on first-pulse, vacuum ignition is primarily a function of the catalyst temperature T_c and the bed configuration. From these tests and from high-speed movies, a catalyst-injector configuration which delivers a uniform distribution of fine hydrazine droplets to the catalyst bed near the injector, e.g., a layer of fine mesh catalyst, appeared to be less susceptible to pressure spiking. Several trends were also inferred from the test results: spiking occurred as often at sea-level as in vacuum; spiking occurred more frequently at T_c less than ambient temperature; ignition delay time θ_i tended to be longer with spiking than without; and decreasing T_c increased θ_i.

In one of the configurations tested, pulverization of the catalyst was observed after a few firings in which peak spike pressures exceeded four times the design pressure. It was hypothesized that this pulverization and spiking might be due to internal pressure in the catalyst granules generated by very rapid decomposition of accumulated hydrazine.

Prefiring immersion of the catalyst in water caused a significant increase in θ_i and produced a rounded P_c trace. Consequently, it is felt that atmospheric moisture absorption by the catalyst is probably not the underlying cause of spiking and catalyst attrition.

Experiments intended to check the effect of outgassing (by measuring P_c and T_c vs vacuum exposure time) led to no conclusions concerning the effect of the outgassing on reaction startup.

Propellant valve leakage must be carefully avoided in vacuum qualification tests.

Some injector clogging was found to be due to the product of a reaction between N_2H_4 and CO_2, which occur after only a brief exposure of N_2H_4 to air. Once formed, the material was insoluble in water, alcohol, acetone, or trichlorethylene. Complete sublimation of this material was obtained by heating to 275°F. Therefore, it is recommended that N_2H_4 be handled under an inert atmosphere.

The results of this investigation indicate that the underlying mechanism (s) of deleterious first-pulse, chamber-pressure spiking is not at all clear and could involve the fundamentals of the N_2H_4 decomposition reactions, which are not fully understood. Further studies concerned with alleviating pressure spiking might first be directed toward acquiring a better understanding of these reactions.

References

[1] Greer, H. and Griep, D. J., "Dynamic Performance of Low-Thrust Cold-Gas Reaction Jets in a Vacuum," *Journal of Spacecraft and Rockets*, Vol. 4, No. 8, Aug. 1967, pp. 983–990.

[2] Carlson, R. A. and Baker, W., "Space Environmental Operation of Experimental Hydrazine Reactors," 4712.4067-28, April 1967, TRW Systems, Redondo Beach, Calif.

[3] Schmitz, B. W. and Smith, W. W., "Development of Design and Scaling Criteria for Monopropellant Hydrazine Reactors Employing Shell 405 Spontaneous Catalyst," RRC-66-R-76, Vols. I and II, Jan. 1967, Rocket Research Corp., Seattle, Wash.

[4] Chu, J. C., "Catalytic Decomposition of Hydrazine," TM-59-0000-945A, Dec. 1959, Space Technology Labs., Redondo Beach, Calif.

[5] Kesten, A. S., "Turbulent Diffusion of Heat and Mass in Catalytic Hydrazine Monopropellant Decomposition," *Journal of Spacecraft and Rockets*, Vol. 7, No. 1, Jan. 1970, pp. 31–36.

[6] Emmett, P. H., ed., *Catalysis*, Vol. I, Reinhold, New York, 1954.

[7] McHale, E. T. et al, "Determination of the Decomposition Kinetics of N_2H_4 Using a Single Pulse Shock Tube," *Tenth Symposium on Combustion*, Combustion Institute, Pittsburgh, Pa., 1965, pp. 341–351.

[8] Gray, P. and Lee, J. C., "Recent Studies of the Oxidation and Decomposition Flames of Hydrazine," *Seventh Symposium on Combustion*, Butterworths Scientific Publications, London, 1959, pp. 61–67.

[9] Antoine, A. C., "The Mechanism of Burning of Liquid Hydrazine," *Eighth Symposium on Combustion*, Williams and Wilkins, Baltimore, Md., 1962, pp. 1057–1059.

[10] Adams, G. K. and Stocks, G. W., "The Combustion of Hydrazine," *Fourth Symposium on Combustion*, Williams and Wilkins, Baltimore, Md., 1953, pp. 239–248.

[11] Eberstein, I. J. and Glassman, I., "Consideration of Hydrazine Decomposition," *AIAA Progress in Astronautics and Rocketry: Liquid Rockets and Propellants*, Vol. 2, edited by L. E. Bollinger et al., Academic Press, New York, 1960, pp. 351–366.

[12] Salvinski, R. J. et al., "Advanced Valve Technology," 06641-6004-R000, Nov. 1966, TRW Systems, Redondo Beach, Calif., p. 5.2.

[13] McAdams, W. H., *Heat Transmission*, McGraw-Hill, New York, 1954, p. 320.

[14] Kennard, E. H., *Kinetic Theory of Gases*, McGraw-Hill, New York, 1938, pp. 291–333.

[15] Audrieth, L. F. and Ogg, B. A., *The Chemistry of Hydrazine*, Wiley, New York, 1951, pp. 212–218.

[16] Prager, B. and Jacobson, P., eds, *Beilstein's Handbook der Organic Chemie*, Vol. III, Edward Brothers, Ann Arbor, Mich., 1943, p. 125.

§§ Reference 15, for example, suggests $CO_2 + 2N_2H_4 \rightarrow N_2H_3 - CO_2N_2H_5$ (carbazic acid hydrazine) or $2CO_2 + N_2H_4 \rightarrow N_2H_2(COOH)_2$ (hydrazidicarboxylic acid). These reactions are not well characterized.[16]